



31 **Keywords**

32 Westerlies, last glacial maximum (LGM), lunette, aeolian, lake levels, palaeolimnology,
33 palaeohydrology, ground penetrating radar (GPR), optically stimulated luminescence (OSL)

34

35 **1 Introduction**

36

37 The temperate latitude westerly wind system influences the southern half of the Australian
38 continent, and influences not only this region's climate but also the formation and response of its
39 landscape systems. Understanding the history of the westerlies in the Australasian region is
40 therefore important for understanding the climate and environmental history of eastern Australia
41 (Shulmeister et al., 2004; Fletcher and Moreno, 2012; Lorrey et al., 2012).

42

43 Here we investigate past wind regime changes in eastern Australia as reflected in the shoreline
44 marginal landforms of the Little Llangothlin Lagoon (LLL). LLL is a presently shallow lake
45 which sits at 30 °S (30° 5' 9"S, 151° 46' 53"E) in northern New South Wales. It lies close to the
46 present day northern boundary of the winter westerlies, therefore providing an excellent
47 opportunity to investigate long-term changes in prevailing wind direction and intensity. The
48 lagoon has a lunette (transverse shoreline dune) on its eastern shoreline and a possible beach
49 berm on its south-eastern margin. These landforms reflect aeolian and wave-driven transport and
50 deposition of sediments, and consequently provide indicators for the orientation of prevailing
51 wind directions and intensity at the time of sediment deposition (Bowler, 1968; Bowler, 1973,
52 1983). In this study we undertook luminescence dating combined with geomorphic and
53 stratigraphic investigations to reconstruct past periods of westerly, and possible north-westerly,
54 prevailing wind flow in this region.

55

56 The endorheic basin was formed in gently undulating tableland comprising Tertiary basalt flows
57 at approximately 1300 m above mean sea level (AMSL). The western shoreline of LLL is
58 dominated by a low ridge of basalt, which rises 30 m above the lake (see Fig 1). On the eastern
59 side of the basin, the lake is bound by a low hill of granite that forms part of the New England
60 Batholith (Shaw and Flood, 1981). The Lagoon covers an area of 1.2 km² and has a catchment



61 of 3.2 km². LLL is a shallow, roughly circular permanent lake with a maximum depth of 2 m
62 that shallows during droughts, which in this part of Australia are often associated with El Nino
63 years. As far as we can determine, the lake has never dried out fully in post-European settlement
64 times (Woodward et al., 2014b). Another, smaller, lake (Billy Bung Lagoon) lies c. 500 m to the
65 southwest of LLL and is separated from the main lake by the low basalt ridge.

66
67

68 The origin of the New England ‘lagoons’ is cryptic. Conraeds (1989) showed that they were
69 associated with former drainage lines that were occupied by basalt flows. He suggested that
70 uneven infilling of former valleys by basalt during the Tertiary produced shallow depressions
71 where the shallow lakes and swamps, locally called ‘lagoons’, formed. Similar lakes have been
72 described elsewhere along the tablelands of the Great Dividing Range and Ollier (1979)
73 suggested a tectonic origin for these features, proposing that uplift of the Eastern Highlands
74 caused back tilting on many streams. Other authors such as Bell et al. (2008) have suggested a
75 deflationary origin, where intense weathering occurred as a result of wetting and drying of the
76 basalt. The mechanisms are not incompatible and deflation may have enhanced and maintained
77 the basins which were created by back-tilting.

78

79 Many of these upland lakes have lunettes on their eastern margins (*sensu* Bowler 1976). These
80 are transverse crescentic ridges dominated by wave action and shoreline drift, with coarse
81 textured wave-built ridges on downwind margins (Bowler, 1986). Their regular outline reflects
82 influence of strong wave action, while the aeolian deflation of sands from the beach forms
83 foreshore dunes with an orientation equivalent to the winter wind resultant vector (Bowler,
84 1971). The proportion of clay and silt in lunettes increases during periods of shoreline
85 regression, and is derived from efflorescence and pelletisation of saline lacustrine sediments on
86 the drying lake floor.

87

88 The catchment is fed by summer rainfall (mean = 880 mm) and has a theoretical net annual
89 moisture balance deficit of c. 400 mm (Woodward et al., 2014a). The regional vegetation is
90 dominated by montane open eucalypt woodland, while the lagoon itself contains extensive beds



91 of tall spike rush *Eleocharis sphacelata* and the water plant *Potamogeton tricarinatus* in the
92 deeper parts of the basin. Other swamp plants, including *Carex glaudichaudiana*, are dominant
93 in the surrounding wet margins of the lagoon.

94
95 The lagoon has been intensively investigated from a palaeoecological and environmental
96 viewpoint because it is a major bird reserve as well as a Ramsar wetland. Furthermore, the site
97 has been identified as a location of exceptional soil erosion since European settlement (Gale et
98 al., 1995; Gale and Haworth, 2005), although this has recently been challenged (Woodward et
99 al., 2011). The site has more recently become a focus for work due to inferred changes to basin
100 hydrology in response to tree clearance during European settlement of the New England
101 Tablelands (Woodward et al., 2014a). There has also been some investigation of the
102 archaeological history of the lagoon suggesting that landscapes such as these provided relatively
103 rich resources for Aboriginal people, and that New England lagoons became the foci for
104 ceremonial activities, although the degree to which hydrological conditions influenced human
105 activity remains poorly understood since chronological control for the pre-European period has
106 so far been lacking (Beck et al., 2015).

107

108 This paper examines the geomorphic context of shoreline features on the western and southern
109 margins of the lagoon and focuses on the history of lake-margin sediment deposition to
110 reconstruct the climatic circulation from the last glacial maximum (LGM) into the Holocene.

111

112 **2 Materials and Methods**

113

114 *2.1 Field investigations*

115

116 Transects across an apparent beach berm and the lunette were surveyed using a MALA ProEx
117 ground penetrating radar (GPR) system with a 500 MHz antenna and integrated high-resolution
118 GPS. The GPR data were collected in transects forming a rough grid parallel and perpendicular
119 to the trend of hypothesised beach and lunette landforms. The GPR was hand-dragged at a speed of
120 ~ 4 kph and fired using time firing at a rate of 10 Hz resulting in an average along-track



121 resolution of 0.11 m and 0.07 m vertical resolution, based on a center frequency of 500 MHz.
122 After acquisition, radar data were processed using GPR Slice software (DC drift; user-defined
123 signal gain; bandpass lo=350 MHz, hi=650 MHz; background removal). Profiles were
124 topographically corrected using elevation data from the GPS system and spot-checked using
125 known elevations. While absolute topography was not reliable, relative elevation was
126 consistently reproducible. Individual profiles were converted to depth-distance using the
127 published radar velocity for wet sands of 0.07 m/ns in the beach ridges and dry sands 0.12 m/ns
128 in the lunette (Neal, 2004). Depth-distance profiles were used to evaluate sediment thickness and
129 observe true geometry of radar reflectors.

130

131 The sub-surface sediments were logged using a hand auger to a depth of between 0.6 m and 1.2
132 m, depending on sub-surface conditions. Sub-samples were collected for grain size analyses.
133 Four samples were collected for optically stimulated luminescence (OSL) dating using steel
134 tubes, wrapped in black plastic, and transported to the Max Planck Institute for Evolutionary
135 Anthropology in Leipzig for analysis.

136

137 *2.2 OSL dating - Equivalent dose measurements*

138 Sample preparation and measurement for OSL dating was undertaken in the luminescence dating
139 laboratory of the Department of Human Evolution, Max Planck Institute for Evolutionary
140 Anthropology in Leipzig. The OSL samples were prepared under subdued red light using
141 published methods (Fitzsimmons et al., 2014). This involved sieving, applying treatments to
142 remove carbonates and organic matter, and isolating pure, 180-212 μm quartz grains. The outer
143 $\sim 10 \mu\text{m}$ alpha-irradiated rind of each grain was removed by etching in hydrofluoric acid, and the
144 sample was then subjected to a final sieve to remove finer fragments which had broken off
145 during etching. The quartz grains were then prepared as small aliquots (18 discs; 1 mm
146 diameter) for preheat testing and as single grains (600 grains; 6 single grain discs) for equivalent
147 dose (D_e) measurement.

148

149 D_e measurements were undertaken using an automated Risø TL-DA-15 equipped with blue light-
150 emitting diodes (for preheat and initial dose estimate testing), and a TL-DA-20 reader with a



151 single grain attachment containing a green laser emitting at 532 nm, for light stimulation of
152 single aliquots and single grains respectively (Botter-Jensen et al., 2000). Irradiation was
153 provided by calibrated $^{90}\text{Sr}/^{90}\text{Y}$ beta sources. Equivalent doses were determined on single grains
154 using the single aliquot regenerative dose (SAR) protocol of Murray and Wintle (2000; 2003).
155 Preheat temperatures of 260°C were chosen based on the results of the preheat plateau tests
156 (Figure S1) for the natural and regenerative doses, with a preheat temperature of 220°C for the
157 test doses (0.94 Gy).

158

159 Individual grains were analysed for their suitability for OSL dating based on the selection criteria
160 of Jacobs and Roberts (2007). The single grain dose distributions of all samples are >40%
161 overdispersed with complex dose populations (Table S1), and therefore the Finite Mixture Model
162 (FMM) was used to identify dose populations (Galbraith and Green, 1990). The OSL dating
163 results are summarised in Table 1. Equivalent dose distributions for the four samples are shown
164 as radial plots, with the FMM-derived dose populations highlighted, in Figure S4.

165

166 *2.3 OSL dating - Dose rate calculations*

167 Uranium, thorium and potassium (^{40}K) activities were measured in the “Felsenkeller” laboratory
168 at VKTA Rossendorf in Dresden, Germany, using low-level gamma-ray spectrometry. Dose
169 rates were calculated using the conversion factors of Stokes et al. (2003) with β -attenuation
170 factors taken from Mejdahl (1979). Beta counting was based on 1 g homogenized subsamples
171 and used for the beta component of the dose rate. Measured water contents ranged from 5-10%
172 and these values were used for all samples. Cosmic dose rates were calculated from Prescott and
173 Hutton (1994).

174

175 **3 Results**

176

177 *3.1 Geomorphology*

178 There are no dune or beach deposits on the western side of the lake (Figure 1). The main
179 geomorphic feature on the eastern side of the lake is a small dune system and the low basalt
180 ridge. The dunefield comprises a north-south oriented ridge less than 2 m high adjacent to the



181 lake, a swale behind that is occupied by a small stream and a small sand flat area that extends up
182 to 50 m east of the lake shore.

183

184 The lunette on the eastern shore is composed of poorly sorted medium sand grading upwards into
185 fine sand with accessory silt contents of 3-15%. Particle size results and other stratigraphic
186 information are plotted on Figure 1. GPR transects are shown in Figures 2a and 2b.

187

188 On the SE margin of LLL, there is a partly infilled outlet, immediately to the west of which is a
189 c. 100 m long, 50 m wide low (< 1m) berm. The berm is poorly to well sorted, medium and
190 coarse quartz rich sand with iron-manganese, pisolithic gravel and a silt content of 1-14%.

191

192 *3.2 GPR results*

193

194 The GPR proved effective at mapping stratigraphic architecture and subsurface character to a
195 depth shallower than 4 m in the berm (Figures 2a and 2b). GPR data suggest the presence of
196 several distinct units related to changes in lake level and the development of spit/barrier and
197 berm formations (Shan et al., 2015; Thompson et al., 2011). The berm showed strong internal
198 stratification on feature perpendicular lines with strong sigmoidal clinoforms indicating beach
199 progradation to the west (Thompson et al., 2011) as well as low-angle sub-parallel reflectors
200 dipping to the east suggesting basin infill via over wash processes. This package is underlain by
201 a convex up package of reflections that are sub-parallel with dips to the east and west.
202 Comparison of this feature with those identified by Shan and others (2015) suggest the complex
203 in underlain by a spit complex. Additional information on the character of the lower units
204 associated with the interpreted spit are unavailable due to the existing GPR data coverage.

205

206 The internal stratigraphy of the fine-grained lunette was difficult to assess with the GPR.
207 Evidence of extensive modern bioturbation by rabbits was observed during the radar acquisition.
208 The shallow penetration did however show weak internal characteristics commonly associated
209 with lunette formation (Thomas and Burrough, in press). These included eastward dipping high
210 angle reflectors that are truncated on the western facing slope, coupled with areas of parallel to



211 sub-parallel reflections that change to steeply dipping reflections. All reflectors are laterally
212 discontinuous and show evidence of disturbance at all depths observed, rendering the GPR data
213 ineffective at determining genetic processes or detailed landform characteristics.

214

215 *3.3 OSL results*

216

217 The OSL age data are summarised in Table 1, and shown with respect to stratigraphy and
218 catchment geomorphology in Fig 1. The three samples collected from three different locations
219 along the lunette suggest that the entire landform was formed during the LGM, between c. 24-19
220 ka. The secondary age populations identified by FMM are all younger than the main phase of
221 deposition (Figure S2) and suggest phases of partial reactivation or pedogenic infiltration of
222 material into the lunette. The younger age populations from sites LL3 and LL4 in the central part
223 of the lunette are comparable and suggest contemporaneous post-depositional infiltration of
224 younger material or partial reactivation of the lunette in the early Holocene (c. 9-8 ka; Table S2).
225 Sample L-EVA 1230 (LL3) exhibits a third peak centred on 11.8 Gy (9.1 ka). The second major
226 age population from the LL2 site in the southern part of the lunette dates to the mid-Holocene
227 (5.6 ± 0.5 ka; Table S2) and suggests spatial and temporal variability in the Holocene post-
228 depositional pedogenesis (or reactivation) of the lunette.

229

230 The overdispersion on individual D_e results from the berm was too high (79.9%; Table S1) to
231 reliably define a depositional age, although the largest age population yields a mid-Holocene age
232 (5.1 ± 0.5 ka; Table 1) comparable with the reactivation of the southern part of the lunette at
233 LL2. The minor dose populations yield ages of 11.1 ± 1.6 ka, 2.3 ± 0.3 ka and 1.2 ± 0.1 ka
234 (Table S2).

235

236 **4 Discussion**

237

238 *4.1 A possible spit/barrier berm on the SE corner of the lagoon*

239



240 The most cryptic landform in the basin is the barrier feature on the SE margins of LLL. The
241 feature was identified by Gale et al. (2005), who interpreted it as part of a relict older lunette
242 feature. From visual observations alone, this is a reasonable interpretation because the low berm
243 does look like the erosional shadow of an older ridge. Our sedimentologic and GPR structural
244 investigations, however, discount this interpretation. Based on both GPR and field observations
245 from pits, the feature is a beach berm, with numerous small wash-over structures (see Fig. 2a).

246

247 The berm barrier feature is composed of pea sized gravels with a finer sandy matrix. We assume
248 the sandy matrix to be post-depositional because it is incompatible with the sedimentary
249 structures and post-depositional infilling of openwork deposits is common. In addition, the
250 contrast between locally sourced detrital basalt gravels and reworked quartz-rich sand and silt is
251 striking. The matrix may have accumulated either through aeolian accession, or through
252 filtration of sands through the barrier during high lake stands when the berm would have acted as
253 a permeable filter for the lake. Given the mostly coarse nature of the matrix (medium to coarse
254 sand), we prefer the two-stage filtration hypothesis.

255

256 The pea-sized gravels are detrital. We suggest that the most likely origin for this feature is as a
257 spit that developed from the basalt ridge on the SW edge of the lake, and that the basalt gravels
258 were moved along the shoreline by longshore drift. The barrier ultimately cut off an area to the
259 SW of the present lake that was part of a larger, ancestral lake feature, for which we have no age
260 constraint due to the lack of associated sedimentary deposits. The luminescence sample based on
261 the finer matrix material yielded a highly dispersed dose distribution with four age populations,
262 which is not unexpected given our hypothesis that the matrix is post-depositional. The grains
263 may represent the accretion of fines to the barrier during high stands in the lake in the early (c.
264 11 ka), mid (c. 5.6 ka) and late Holocene (c. 2.3 ka, 1.2 ka).

265

266 *4.2 Aeolian history of LLL from the lunette*

267

268 Based on the morphology, sedimentary composition and internal structure, the feature along the
269 eastern shoreline of LLL is clearly a composite beach and aeolian landform. The quartz-rich



270 sands were most likely derived from the granites on the eastern side of the catchment, which
271 deposited into the lake and were subsequently reworked onto the shoreline. Curiously, even
272 though half the basin is comprised of basalt, there is little evidence for basalt-derived sediments
273 in the lunette system. By contrast, the fine sediments in the depocentre of the lake basin are
274 primarily derived from basalt (e.g. Woodward et al., 2011). This implies that there is an effective
275 sorting mechanism within the basin. The obvious candidate for this process is wind-blown
276 waves.

277

278 Present day wind roses for LLL (BOM, 2014) demonstrate that there are two primary wind
279 directions (Figure 4), one from the east and the other from the west to north-west. These
280 prevailing winds have strong seasonal components. Winter winds (August) are dominated by
281 westerlies and provide the strongest and most persistent flows (8% calm) consistent with
282 eastward transport and deposition of sediments onto a lunette situated on the eastern shoreline of
283 LLL. Summer winds (February) are dominated by easterlies associated with onshore circulation
284 on the northern limb of the sub-tropical high pressure cell in summer (Fig. 4). These easterly
285 winds are on average weaker (20% calm) but do include short periods of relatively high intensity
286 winds which might be expected to result in sediment transport to, and deposition onto, the
287 western side of the lake. It is curious therefore that all depositional landforms marginal to LLL
288 are located on the east and south-east sides of the lake, with no deposition on the western
289 shoreline. This indicates that the most effective net sand-transporting wind, associated with
290 lunette and berm formation, was from the west/north-west. The transport is most likely to have
291 been primarily sub-aqueous, since the relatively poor sorting in the foredune indicates only
292 intermittent aeolian transport, at least of the coarsest component.

293

294 One obvious question is why the westerlies are so strongly recorded in the LLL lunette, and not
295 the easterlies. This partly reflects the greater frequency of high wind speeds from the west, but
296 on its own it is unlikely to explain the entire phenomenon. The most parsimonious answer
297 integrates the sedimentary information with seasonal variations in the biological system. The
298 rush beds occurring in the shallower parts of the lake are most fully developed during the
299 summer. Unlike much of Australia, winters are severe on the New England Tablelands due to the



300 relatively high elevations, and seasonal die-back of the jointed wire rush is also observed today.
301 New growth emerges in spring and dies off in autumn in cooler, high altitude sites (Rajapaskse et
302 al., 2006). Consequently, the summer peak in vegetation cover disrupts the wind fetch over the
303 lake precisely at the same time as the easterly winds penetrate the tablelands, thereby reducing
304 the ability for waves to set up during the warmer months.

305

306 The luminescence ages from the lunette are coherent; all three samples are dominated by grains
307 that are LGM in age. The samples all overlap at 2σ and produce a mean age of 21.5 ka,
308 indicating that the main phase of dune activity at LLL occurred during the LGM. Our
309 interpretation that the dominant sediment transport mechanism was subaqueous therefore implies
310 that the LGM oversaw permanent, and probably full, lake conditions at LLL. Evidence from
311 pollen records and sedimentary archives from the depocentre of the lake support our hypothesis
312 for a full lake during the late LGM (c. 19 ka). Our argument for the persistence, and perhaps
313 intensification, of winter westerlies throughout the LGM at LLL is also confirmed by
314 observations made at North Stradbroke Island some 300 km to the north-northeast of our site
315 (Petherick et al., 2009; McGowan et al. 2009). North Stradbroke Island lies at the very northern
316 edge of the westerlies zone, and the accession of fine aeolian material into a dune lake there
317 indicates that the winter westerlies were operative at the LGM in South East Queensland at
318 27.20°S (Petherick et al., 2009; McGowan et al. 2009).

319

320 A secondary peak in grain ages is observed from all three lunette samples. This peak is less well
321 defined but in all three cases relates to the early to mid-Holocene between 9 and 6 ka. Work from
322 the lake (Woodward et al., 2011) has already demonstrated that the early Holocene was the last
323 phase, before the modern anthropogenically modified lake, with lake full conditions as
324 represented by extensive *Eleocharis* beds. We infer partial reactivation at this times.

325

326 We note a third grain age peak in one lunette sample (EVA1230) at c. 3 ka. This is both the
327 weakest individual age peak and not replicated at any other site. It is possible that this represents
328 a dune re-activation event, bioturbation, or even aboriginal usage of the site which has been
329 proposed to have intensified during the late Holocene (post 4300 yr; Beck et al., 2015). At this



330 stage this event, if real, is still poorly controlled chronologically and we do not interpret it
331 further.

332

333 Overall, our evidence demonstrates that at the LGM, winter westerly winds were strong enough
334 to form the eastern shoreline lunette in a single phase, with possible later reactivation during the
335 early Holocene. Critically, dune activation depends as much on high water levels in the lake as it
336 does on sand mobilizing winds (Bowler, 1983). During the Pleistocene, elevations above 800 m
337 in the region were subject to extensive, active development of block deposits, screens, and
338 solifluction lobes, indicating winter cooling of at least 10.5 °C relative to present (Slee and
339 Shulmeister, 2015). Reduced evaporation at this time is likely to have been sufficient to cause
340 the change to a positive hydrological balance in the lake.

341

342 For the intervening periods at least in the Holocene, the evidence (Woodward et al., 2014a)
343 suggests that water levels were lower and/or even that the lake was ephemeral. It is highly
344 unlikely that sand would be transported to the high stand beach during low lake levels. If the
345 entire basin floor fully dried out, pelletised clays might be expected, and yet none are observed.
346 There are two likely reasons for this. Firstly, this high elevation site is unlikely to become very
347 arid even during dry phases when swampy conditions probably persisted on the basin floor.
348 Similarly, it is unlikely that salt formation is significant in this setting and clay pelletisation may
349 not occur. This is similar to observations from Lake George, which also occurs in a cool
350 temperate climate setting along the Dividing Range (Fitzsimmons and Barrows, 2010).

351

352 In summary, these records strongly suggest that for the two intervals recorded (the LGM and
353 early Holocene), the overall circulation conditions at LLL were very similar to the present day.
354 This region presently lies near the northern limit of westerly penetration in winter. Westerlies
355 occurred during both the early Holocene and the LGM suggesting that at both time intervals the
356 position of the westerly jet lay near 30°S, which is its modern track. For the intervening periods,
357 absence of evidence is not evidence of absence and if the winter westerly lay at this latitude
358 during peak warming in the early Holocene and during the LGM, it seems reasonable to suppose
359 that this track has been persistent over the last 25 ky.



360

361 One possibility is that the westerly lay north of its current track during the LGM and that the
362 timing of the westerlies at LLL shifted seasonally. A northward shift of $\sim 3^\circ$ (350 km) in the
363 position of the westerly wind belt during MIS 2 was recorded in sediments from marine cores in
364 the Tasman Sea (Hesse, 1994). Analysis of the aeolian component of lake sediments on North
365 Stradbroke Island at 27°S for the period 25-22 ka indicates dust sources in the SW Murray-
366 Darling Basin, with a secondary component from WNW of the site (Petherick et al. 2009). This
367 lends support to a possible northward shift in the westerlies.

368

369 **Conclusions**

370

371 This study indicates that westerly winds constructed a foredune ridge at LLL during the LGM
372 under the influence of high lake levels. This ridge was reactivated during high lake stands in the
373 early to mid-Holocene. The persistence of westerly winds at this site during the LGM confirms
374 observations from North Stradbroke Island at the northern limits of penetration of the temperate
375 latitude westerlies. This suggests that the overall circulation pattern in this part of eastern
376 Australia, at the modern northern limits of westerly winter flow, remained constant during both
377 the LGM and the early Holocene. Overall, this points to minimal change in circulation patterns
378 over the last 25 ky.

379

380 **Team List**

381 James Shulmeister

382 Justine Kemp

383 Kathryn Fitzsimmons

384 Allen Gontz

385

386 **Copyright Statement**

387

388 Except where explicitly acknowledged the authors hold the copyright of the materials presented.

389



390 **Author Contributions**

391 J Shulmeister lead the project, assisted with field sampling for OSL and grain size and lead the
392 manuscript development. J Kemp assist in the field with OSL sample acquisition, conducted
393 grain size analysis and participated in manuscript development. K Fitzsimmons oversaw the OSL
394 sample analysis and participated in manuscript development. A Gontz lead the GPR acquisition
395 and processing, assisted with OSL sampling and manuscript development.

396

397 **Acknowledgements**

398 This research was funded by an Australian Research Council Discovery Grant DP110103081,
399 “The last glaciation maximum climate conundrum and environmental responses of the Australian
400 continent to altered climate states”. We thank S. Hesse for assistance with OSL sample
401 preparation. C. Woodward, J. Chang, and A. Slee assisted with fieldwork. We thank NSW
402 Parks and Wildlife Service for access to the site and the local farmers for retrieving our vehicle
403 from the bottomless suck hole!

404

405 **References**

- 406 Bell, D.M., Hunter, J.T., and Haworth, R.J.: Montane lakes (lagoons) of the New England
407 tablelands bioregion, *Cunninghamia*, 10, 475-492, 2008.
- 408 Beck, W., Haworth, R., and Appleton, J.: Aboriginal resources change through time in New
409 England upland wetlands, south-east Australia, *Archaeol Ocean*. 50, 47-57, 2015.
- 410 Botter-Jensen, L., Bulur, E., Duller, G.A.T., and Murray, A.S.: Advances in luminescence
411 instrument systems, *Radiat Meas*, 32, 523-528, 2000.
- 412 Bowler, J.M.: Aridity in Australia: age, origins and expression in aeolian landforms and
413 sediments, *Earth Sci Rev*, 12, 279-310, 1976.
- 414 Bureau of Meteorology. Summary statistics Guyra Hospital. Climate Data Online. 2014.
415 Available at: http://www.bom.gov.au/climate/averages/tables/cw_056229.shtml. Last accessed.
416 29 February, 2016.
- 417 Coenraads, R.R.: Evaluation of the natural lagoons of the Central Province, NSW—Are they
418 sapphire-producing maars?, *Explor Geophys*, 20, 347-363, 1989.



- 419 Fitzsimmons, K.E., and Barrows, T.T.: Holocene hydrologic variability in temperate
420 southeastern Australia: An example from Lake George, New South Wales, *The Holocene* 20,
421 585-59, 2010.
- 422 Fitzsimmons, K.E., Stern, N., and Murray-Wallace, C.V.: Depositional history and archaeology
423 of the central Lake Mungo lunette, Willandra Lakes, southeast Australia, *J Archaeol Sci* 41, 349-
424 364, 2014.
- 425 Fletcher, M.S., and Moreno, P.I.: Have the Southern Westerlies changed in a zonally symmetric
426 manner over the last 14,000 years? A hemisphere-wide take on a controversial problem,
427 *Quaternary Int*, 253, 32-46, 2012.
- 428 Galbraith, R.F., and Green, P.F.: Estimating the component ages in a finite mixture, *Nucl Tracks*
429 *Rad Meas* 17, 197-206, 1990.
- 430 Gale, S.J., Haworth, R.J., and Pisanu, P.C.: The 210 Pb chronology of late Holocene deposition
431 in an eastern Australian lake basin, *Quaternary Sci Rev*, 14, 395-408, 1995.
- 432 Gale, S.J., and Haworth, R.J.: Catchment-wide soil loss from pre-agricultural times to the
433 present: transport-and supply-limitation of erosion. *Geomorphology*, 68, 314-33, 2005.
- 434 Haworth, R.J., Gale, S.J., Short, S.A., and Heijnis, H.: Land use and lake sedimentation on the
435 New England tablelands of New South Wales, Australia, *Aust Geogr*, 30, 51-73, 1999.
- 436 Hesse, P.P.: The record of continental dust from Australia in Tasman Sea sediments, *Quaternary*
437 *Sci Rev*, 13, 257-72, 1994.
- 438 Jacobs, Z., and Roberts, R.G.: Advances in optically stimulated luminescence dating of
439 individual grains of quartz from archeological deposits, *Evol Anthropol*, 16, 210-223, 2007.
- 440 Lorrey, A.M., Vandergoes, M., Almond, P., Renwick, J., Stephens, T., Bostock, H., Mackintosh,
441 A., Newnham, R., Williams, P.W., Ackerley, D., and Neil, H.: Palaeocirculation across New
442 Zealand during the last glacial maximum at~ 21 ka, *Quaternary Sci Rev*, 36, 189-213, 2012.
- 443 McGowan, H.A., Petherick, L.M., and Kamber, B.S.: Aeolian sedimentation and climate
444 variability during the late Quaternary in southeast Queensland, Australia, *Palaeogeog, Palaeocl*,
445 265, 171-81, 2008.
- 446 Mejdahl, V.: Thermoluminescence dating: beta-dose attenuation in quartz grains, *Archaeometry*
447 21, 61-72, 1979.
- 448 Murray, A.S., and Wintle, A.G.: Luminescence dating of quartz using an improved single-aliquot
449 regenerative-dose protocol, *Radiat Meas*, 32, 57-73, 2000.



- 450 Murray, A.S., and Wintle, A.G.: 2003. The single aliquot regenerative dose protocol: potential
451 for improvements in reliability, *Radiat Meas*, 37, 377-381, 2003.
- 452 Neal, A.: Ground penetrating radar and its use in sedimentology: principles, problems and
453 progress, *Earth Sci Rev*, 66, 261-330, 2004.
- 454 Ollier, C.D.: Evolutionary Geomorphology of Australia and Papua: New Guinea, *T I Brit Geog*,
455 4, 516-39, 1979.
- 456 Petherick, L.M., McGowan, H.A., and Kamber, B.S.: Reconstructing transport pathways for late
457 Quaternary dust from eastern Australia using the composition of trace elements of long traveled
458 dusts, *Geomorphology*, 105, 67-79, 2009.
- 459 Prescott, J.R., and Hutton, J.T.: Cosmic ray contributions to dose rates for luminescence and
460 ESR dating: Large depths and long term variations, *Radiat Meas*, 23, 497-500, 1994.
- 461 Rajapakse L., Asaeda, T., Williams, D., Roberts, J., and Manatunge, J.: Effects of water depth
462 and litter accumulation on morpho-ecological adaptations of *Eleocharis sphacelata*, *Chem Ecol*,
463 22, 47-57, 2006.
- 464 Shan, X., Yu, X., Clift, P.D., Tan, C., Jin, L., Li, M, and Li, W.: The ground penetrating radar
465 facies and architecture of a paleo-spit from Huangqihai Lake, North China: implications for
466 genesis and evolution, *Sediment Geol*, 323, 1-14, 2015.
- 467 Shaw, S.E., and Flood, R.H.: The New England Batholith, eastern Australia: geochemical
468 variations in time and space, *J Geophys Res-Sol Ea*, 86, 10530-10544, 1981.
- 469 Shulmeister, J., Goodwin, I., Renwick, J., Harle, K., Armand, L., McGlone, M.S., Cook, E.,
470 Dodson, J., Hesse, P.P., Mayewski, P., and Curran, M.: The Southern Hemisphere westerlies in
471 the Australasian sector over the last glacial cycle: a synthesis, *Quaternary Int*, 118, 23-53, 2004.
- 472 Slee, A., and Shulmeister, J.: The distribution and climatic implications of periglacial landforms
473 in eastern Australia, *J Quaternary Sci*, 30, 848-58, 2015.
- 474 Stokes, S., Ingram, S., Aitken, M.J., Sirocko, F., Anderson, R., and Leuschner, D.: 2003.
475 Alternative chronologies for Late Quaternary (Last Interglacial–Holocene) deep sea sediments
476 via optical dating of silt-sized quartz, *Quaternary Sci Rev*, 22, 925-941, 2003.
- 477 Thomas, D.S.G., and Burrough, S.L.: Luminescence-based chronologies in southern Africa:
478 analysis and interpretation of dune database records across the subcontinent, *Quaternary Int*, 1-
479 16, in press.



- 480 Thompson, T.A., Lepper, K., Endres, A.L., Johnston, J.W., Baedke, S.J., Argyilan, E.P., Booth,
481 R.K., and Wilcox, D.A.: Mid Holocene lake levels and shoreline behaviour during the Nipissing
482 phase of the upper Great Lakes at Alpena, Michigan, USA, *J Great Lake Res*, 37, 567-576, 2011.
- 483 Woodward, C., Chang, J., Zawadzki, A., Shulmeister, J., Haworth, R., Collecutt, S., and
484 Jacobsen, G.: Evidence against early nineteenth century major European induced environmental
485 impacts by illegal settlers in the New England Tablelands, south eastern Australia, *Quaternary*
486 *Sci Rev*, 30, 3743-3747, 2011.
- 487 Woodward, C., Shulmeister, J., Bell, D., Haworth, R., Jacobsen, G., and Zawadzki, A.: A
488 Holocene record of climate and hydrological changes from Little Llangothlin Lagoon, south
489 eastern Australia, *The Holocene*, 6:0959683614551218, 2014a.
- 490 Woodward, C., Shulmeister, J., Larsen, J., Jacobsen, G.E., and Zawadzki, A.: The hydrological
491 legacy of deforestation on global wetlands, *Science*, 346, 844-7, 2014b.
- 492
- 493

494 **Tables**495 **Table 1.** Equivalent dose (D_e), dose rate data and OSL age estimates for Lake Little Llangothlin.

496 Dose rates are listed as attenuated based on published factors (Stokes et al. 2003; Mejdahl 1979).

Sample	D_e (Gy)	K (%)	Th (ppm)	U (ppm)	Beta dose rate (Gy/ka)	Cosmic dose rate (Gy/ka)	Water content (%)	Total dose rate (Gy/ka)	Age (ka)
L-EVA 1228 (LL1)	6.1±0.6	0.53±0.02	4.0±0.2	1.3±0.1	0.6±0.1	0.19±0.02	10±3	1.21±0.07	5.1±0.5
L-EVA 1229 (LL2)	19.2±0.4	0.34±0.02	3.5±0.2	1.3±0.1	0.5±0.1	0.18±0.02	5±3	1.02±0.06	18.9±1.2
L-EVA 1230 (LL3)	26.9±0.9	0.69±0.04	3.0±0.1	1.3±0.1	0.7±0.1	0.18±0.02	7±3	1.30±0.08	20.6±1.4
L-EVA 1231 (LL4)	22.9±1.2	0.56±0.02	2.7±0.1	0.7±0.1	0.5±0.1	0.18±0.02	6±3	0.98±0.05	23.4±1.8

497

498



499 **Figure Legends**

500 **Figure 1.** Geomorphology and sediments at Little Llangothlin Lagoon (30° 5' 9"S, 151° 46'
501 53"E), 18 km NE Guyra, NSW, showing the locations of GPR transects, sediment cores (right)
502 and the position of OSL samples.

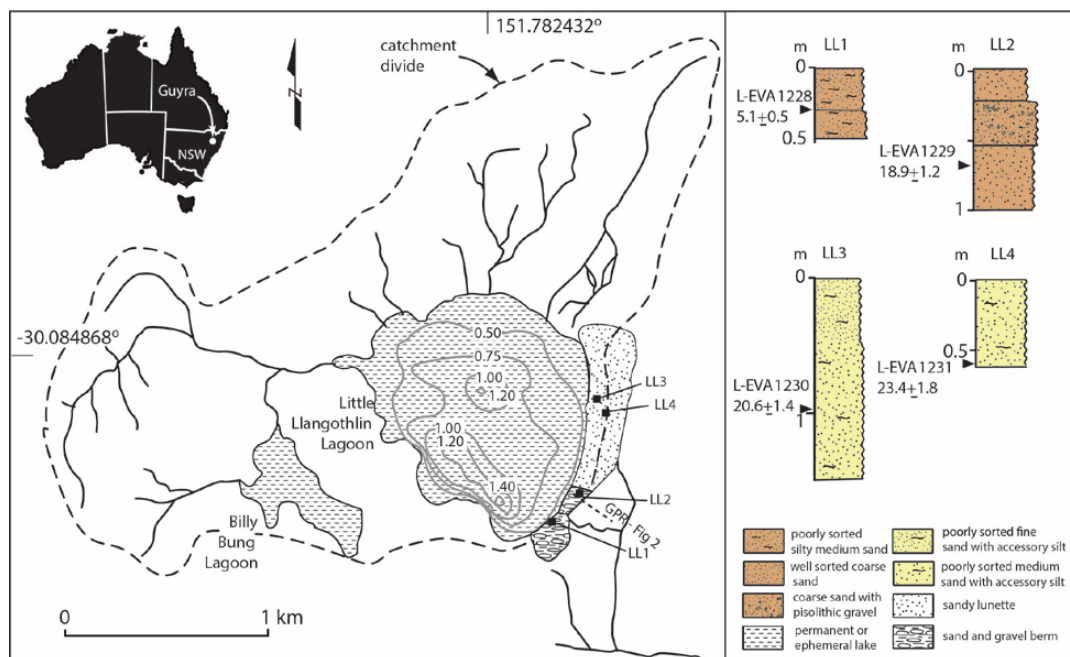
503 **Figure 2a.** GPR transects over the “berm”. See Fig 1. for location of transect. GPR line A7 was
504 acquired perpendicular to the shoreline starting just lakeward of the highest point on the berm.
505 Internal structures are characteristic of an interfingering beach-washover-basin fill sequence over
506 a spit complex. Upper panel, raw data; lower panel, interpretation.

507 **Figure 2b.** GPR line A9 was acquired from the lake shore to the highest point on the berm.
508 Internal structures show characteristics of a beach environment over a spit complex. Top left
509 panel, raw data; top right panel, interpretation. The lower panel shows a conceptual model based
510 on composite GPR profiles suggesting a lower lake facies with spit facies underlying beach,
511 washover and basin fill facies.

512 **Figure 3.** Equivalent dose distributions for the LLL samples, illustrated as radial plots. The
513 shaded populations in each case represent the dominant age peaks; the lines illustrate the other
514 identified populations.

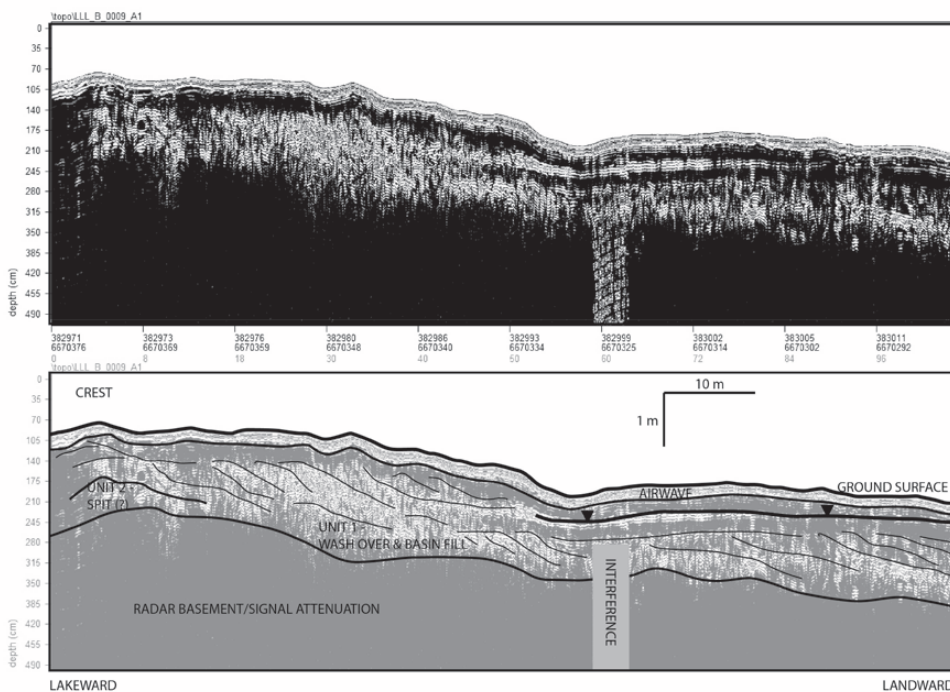
515 **Figure 4.** Rose of 9am wind direction vs wind speed in km/hr at Guyra Hospital, 1332 m AMSL
516 (Bureau of Meterology, 2014).

517



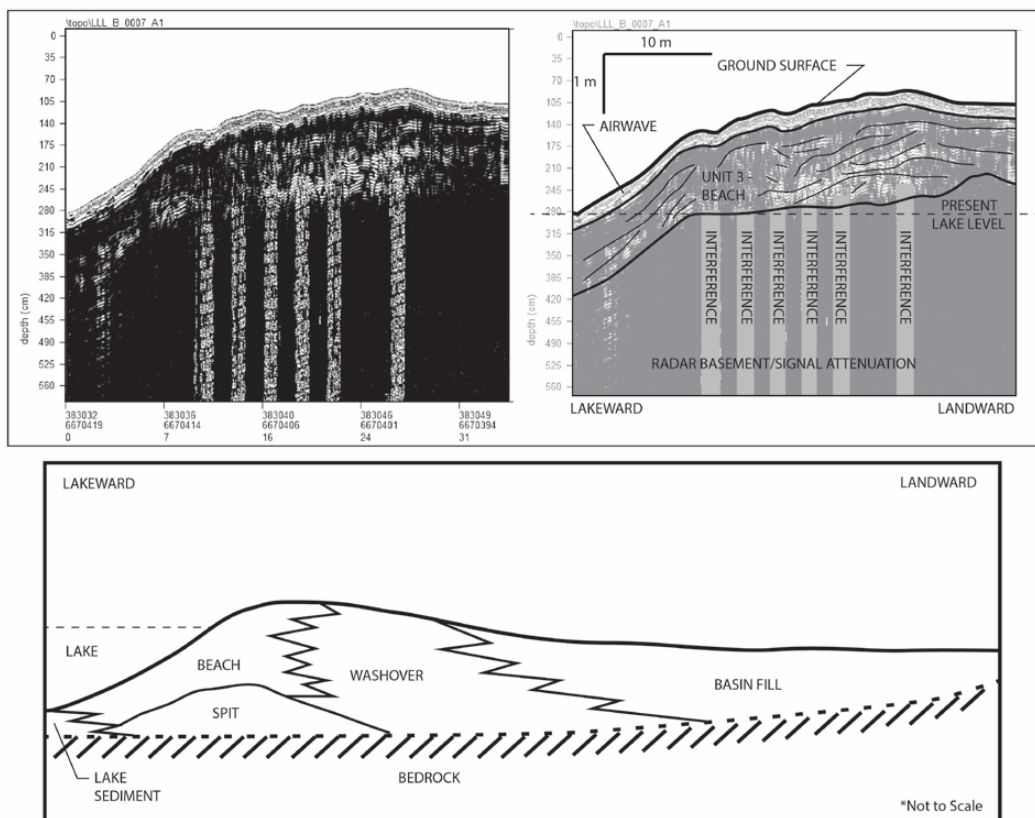
518
 519
 520

Figure 1



521

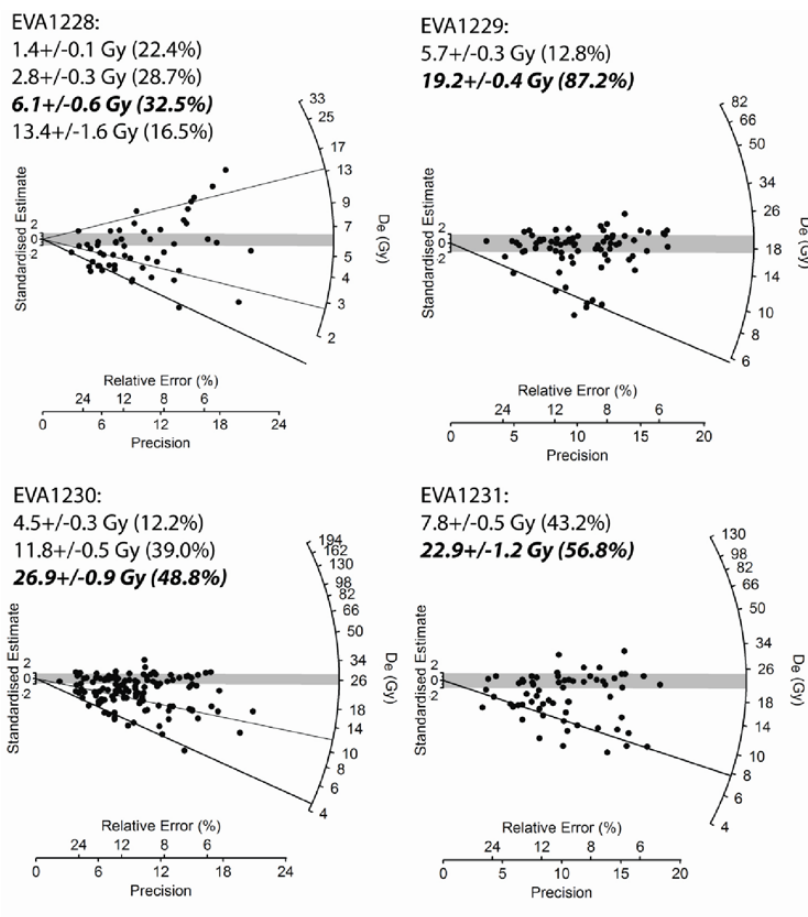
522 **Figure 2a**



523

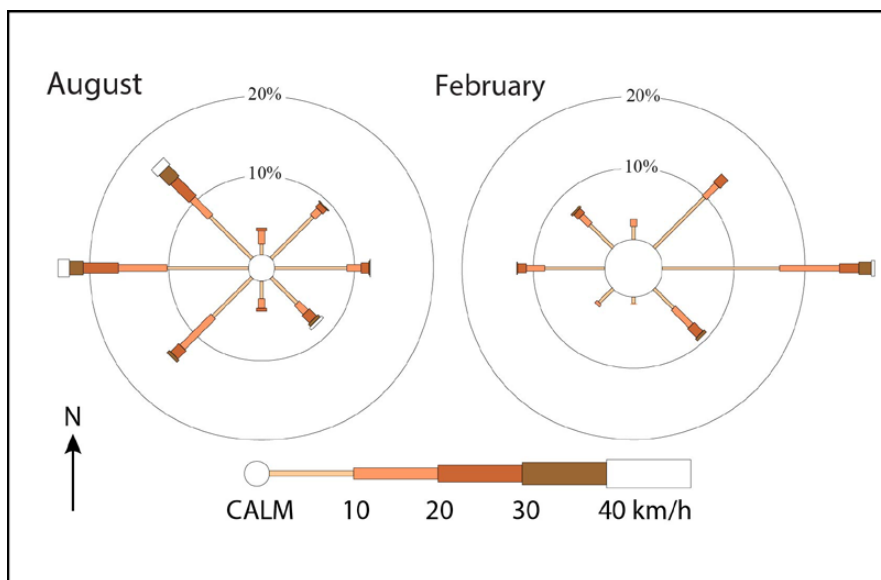
524 **Figure 2b**

525



526
527
528

Figure 3



529

530 **Figure 4**

531